QUENCH AND HIGH FIELD Q-SLOP STUDIES USING A SINGLE CELL CAVITY WITH ARTIFICIAL PITS*

Yi Xie†, Matthias Liepe and Georg Hoffstaetter
Cornell Laboratory for Accelerator-Based Sciences and Education (CLASSE),
Cornell University, Ithaca, NY 14853, USA

Abstract

Surface defects such as pits have been identified as some of the main sources of limitations of srf cavity performance. A single cell cavity was made with 30 artificial pits in the high magnetic field region to gain new insight in how pits limit the cavity performance. The test of the pit cavity showed clear evidence that the edges of two of the largest radius pits transitioned into the normal conducting state at field just below the quench field of the cavity, and that the quench was indeed induced by these two pits. Insights about quench and non-linear rf resistances will be presented.

INTRODUCTION

Pit-like structures on the niobium surface of srf cavities have been shown to cause thermal breakdown under certain conditions [1]. Thus we need to understand better how pits cause quench and what the relevant parameters are. This can be done experientially and by simulating pits. However, the field at which quench is caused by a pit defect varies significantly from pit to pit, and frequently, pits do not cause quench up to the maximum field obtained. Previous thermal feedback models treat pits as normal conducting disks assuming the entire pit area is normal conducting starting from low field [1]. However, real pit-like defects observed in srf cavities have a complex 3-dimensional shape which can not be simply treated as a all normal conducting disk. Recent electromagnetic simulations show that the magnetic field enhancement (MFE) effect is present at the sharp edge or corner of a pit. It was calculated that a pit MFE factor β shows a $(r/R)^{-1/3}$ dependence, where r is the radius of the pit edge and R is the radius of the pit [2]. Therefore a more accurate ring-type defect model in which only pit edges get normal conducting above a certain magnetic field level was developed [3].

Previous experimental studies depended on random data sets collected from pits occasionally found on srf cavities. In order to systematically study the nature of pit-induced quench, a single-cell niobium srf cavity with many artificially drilled pits with different sizes was prepared and tested. Thermometers attached outside the cavity pit locations recorded heating signals as function of the rf magnetic field level.

* Work supported by NSF and Alfred P. Sloan Foundation.
† yx39@cornell.edu, now at Euclid Techlabs LLC.

Table 1: Pit parameters for the pits cavity

Total number of pits	30
Pits radii	200, 300, 400, 600, 750 μm
Pits edge radii	initially unknown
Pits depth	1.5 mm
Pits position	1 inch from the cavity equator

PITS CAVITY DESIGN AND FABRICATION

A single cell 1.3 GHz niobium cavity of the Cornell ERL center cell shape was fabricated. Prior to joining the two halves of the cavity by electro beam welding, 30 pits of various radii were drilled into the inside niobium wall in the high magnetic field region of the cavity, each 1.5 mm deep, which is half of the wall thickness of the cavity. Fig. 1 shows the fabricated half cup with different sizes of pits. In order to obtain different MFE factors of the artificial pits,

Figure 1: Half cup of the pit cavity after drilling of the pits.

pit of 5 different radii R were drilled perpendicular to the cavity wall, with six copies of each size. After drilling the pits and after final electron beam welding of the equator to join the two cavity halves, a heavy BCP of about 120 μm was applied to the pits cavity. This BCP process determined the pits edge radius r along with the different drill sizes used. The parameters of the pits are summarized in Table. 1. In order to use the Cornell single-cell temperature mapping system to record the rf heating from the pits, the pit position pattern is matched to thermometry sensor positions.

ISBN 978-3-95450-122-9

PIT CAVITY EXPERIMENTAL RESULTS

After fabrication, the cavity with the 30 drilled pits of various radii received a 120 μm BCP, was high pressure water rinsed and dried for assembly to the test insert in a class 10 clean room, and received a final 120°C in-situ bake.

RF Test Results

Before the quench, a mild Q-drop effect appeared above 300 Oe. There is a sudden drop in Q_0 at about 520 Oe, followed by a strong Q-slope. As we will discuss later, at this field the local, enhanced magnetic field at the first pit edge reaches the critical magnetic field and the edge starts to transition into the normal conducting state, thereby decreasing the cavity's quality factor. No x-rays were registered and thus no field emission was present during the test.

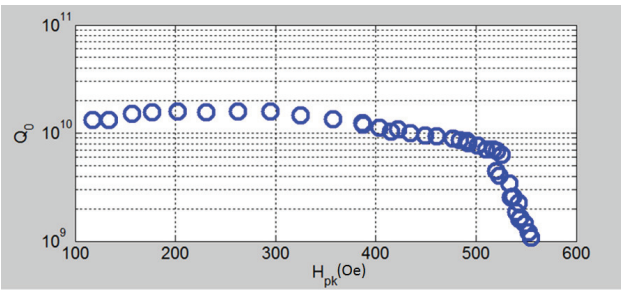

Figure 2: The pits cavity quality factor Q_0 versus the peak surface magnetic field H_{pk} at 1.6 K. The surface magnetic field on the horizontal axis is the peak surface field of the cavity, not taking into account the local field enhancement by the pits.

Temperature Map Results

The single-cell T-map system was used to measure the rf heating at the pits locations as function of magnetic field during the entire cavity rf test. Before temperature maps of all the thermometers were taken, three calibrated Cernox thermometers placed inside the helium bath were used to calibrate the T-map from 4.2 K to 1.6 K at an interval of 0.1 K. After calibration, temperature maps were taken at different fields up to the quench field of the cavity. The uncertainty in ΔT is $\pm$ 1 mK. As an example, Fig. 3 shows one T-map taken at the cavity maximum surface magnetic field of 350 Oe. The row of resistors #9 is at the equator of the cavity. The 38 boards are spaced equally around the cavity. The artificial pits are located at the following positions of the T-map:

- Resistor number 6 and 12;
- Board number (2,4,6); (8,10,12); (14,16,18); (20,22,24); (26,28,30);

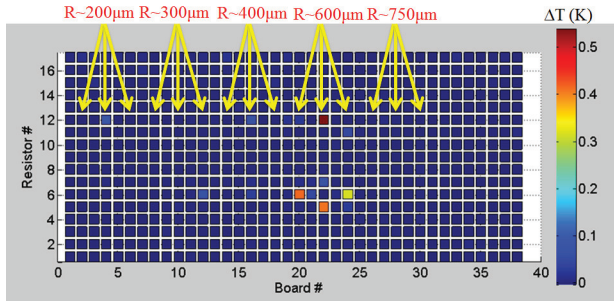

Figure 3: T-map taken at H_{pk} of 350 Oe. Plotted here are ΔT between rf on and off. Note that the T-map data shows good correlation between the heating pattern and the position of the pits.

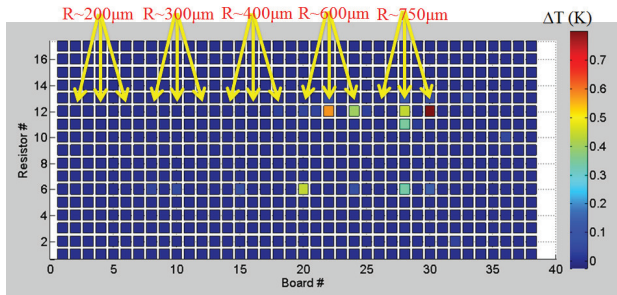

Figure 4: T-map taken at H_{pk} of 500 Oe. Plotted here are ΔT between rf on and off. Note the heating gets larger as compared to the heating at 350 Oe shown in Fig. 3.

As pits cavity maximum surface magnetic field increases, the heating pattern keeps nearly the same and the heating get stronger as can be seen in Fig. 4, which shows the T-map taken around 500 Oe.

From this T-map data, we can conclude that:

- T-map heating pattern does correlate well with the pattern of the actual artificial pit positions on the inner cavity surface.
- Smaller diameter pits show smaller heating and larger diameter pits show larger heating in general. This is in agreement with the a simple magnetic field enhancement model, which predicts that the local magnetic field enhancement at the edges of the pits scales with the radis R of the pits according to $R^{1/3}$ [2], assuming that the edges of all pits have the same sharpness. Accordingly, larger pits will have higher local fields, thus larger rf heating.

The two pits # 22 and #30 were found to cause quench. Fig. 5 shows the heating versus magnetic field of the two quench pits #22 and #30. Both of the two pits show gradual heating until the temperature suddenly jumps to about $\sim$ 1 K at a cavity maximum magnetic field around 545 Oe, which is smaller than cavity quench field of 550 Oe. Note that both pits are among the largest radius pits, which are

expected to have the largest magnetic field enhancement [2].

What likely happened here for the two quench causing pits is that the local, enhanced field at pit edge reached the critical (superheating) magnetic field at given temperature, so part of the pit turned normal conducting. Thus the T-map sensors showed a sudden increase of temperature up to $\sim$ 1 K and also the cavity quality factor Q_0 decreased significantly. The cavity did not quench at this field and did go to a bit higher in the field before quench occurred. So it is clear that the normal conducting edge of pit is initially stable until the field is too high.

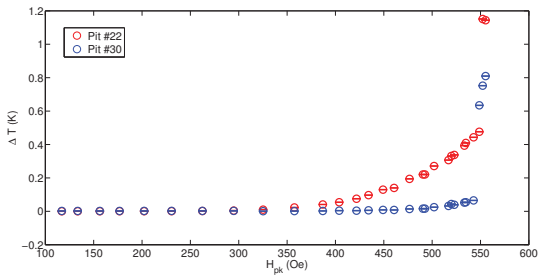

Figure 5: Heating of pit #22 and #30 versus the cavity maximum surface field H_{pk}. Notice the sudden jumps in ΔT at $\sim$ 540 Oe, corresponding to the sudden change in Q_0 at the same field; see Fig. 2.

In addition to the two quench causing pits verified by T-map sensors, there are 9 pits that do not cause quench, but still showed measurable heating signals. Assuming there is magnetic field enhancement at these pit edges, the temperature rise information versus real local magnetic field can provide new valuable information about the high field Q-slope. Fig. 6 shows one of these heating signals from pit #19. For pit #19, below field level of $\log(H_{pk}/Oe) < 4.6$, the pit heating signal is so small that it is below noise level. Within the field range of $5.6 < \log(H_{pk}/Oe) < 6.2$, the heating signal obeys a power law with an exponent of 8. Above field level of $\log(H_{pk}/Oe) > 6.2$, the heating signal does not show an abrupt jump as those pits that induce cavity quench but rather increases more slowly with a power law of an exponent of 4. The maximum heating is about 450 mK when the cavity quenches.

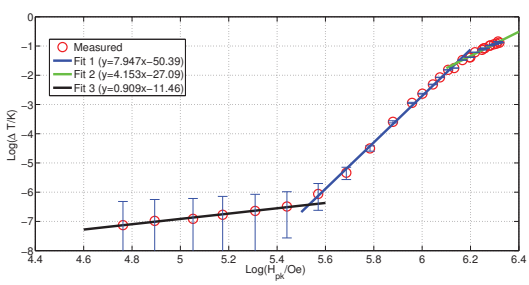

Figure 6: Measured heating signals versus magnetic field for pit #19 with a drill bit radius of 600 μm.

The following observations can be made based on the slope of the pit heating signals.

- At low field, the heating is proportional to H^2, as one would expect for ohmic heating;
- At higher fields, there is clear transition to a strong non-linear behavior, with a final slop of $\log(\Delta T/K)$ versus $\log(H_{pk}/Oe)$ of 4 to 5 at highest fields. This points to a strong field dependence of the BCS surface resistance, for local fields in the 1000 $\sim$ 2000 Oe region at the edges of the pits. It should be noted here that the situation is rather complex, since only a small area at the pit edge is at high fields, and it is not uniform. Nevertheless, from the slope information one concludes that the BCS surface resistance scale with the magnetic field to a power of 4 to 6 at medium fields, and with a power of $\sim$ 2 of the high fields above 1300 Oe.
- The transition to field dependent surface resistance happens at fields similar to where the high field Q-slope starts in BCP cavities ($\sim$ 900 Oe), taking into account the MFE at the pit edges;
- The pit heating data shows that a BCS cavity surface can reach high fields close to the superheating field. The strong Q-slope found in BCS cavities above $\sim$ 900 Oe thus is likely caused by a combination of a non-linearity of the BCS surface resistance and thermal feedback caused by the increased rf losses over a larger area. For the pit edges, the high field area is very small, so the total power disposed is small and thermal feedback is less important.

CONCLUSIONS

a single cell cavity with 30 artificial pits in the high magnetic field region was made to gain new insight in how pits limit the cavity performance. The test of the pit cavity showed clear evidence that the edges of two of the largest radius pits transitioned into the normal conducting state at a field just below the quench field of the cavity, and that the quench was indeed induced by these two pits. The pits also give some new insight into the non-linear surface resistance of niobium at high fields.

REFERENCES

[1] Y. Xie, H. Padamsee, A. Romanenko. Relationship Between Defects Pre-Heating and Defects Size. SRF2009, Berlin, Germany.

[2] V. Shemelin, H. Padamsee. Magnetic field enhancement at pits and bumps on the surface of superconducting cavities. SRF Report 080903-04, Cornell University.

[3] Yi Xie, M. Liepe, H. Padamsee. Thermal modelling of ring-type defects. SRF2009, Berlin, Germany.

ISBN 978-3-95450-122-9